Efficacy of Crosslinking on Tailoring *In Vivo* Biodegradability of Fibro-porous Decellularised Extracellular Matrix and Restoration of Native Tissue Structure: A Quantitative Study using Stereology Methods

Krishna Burugapalli[1,2], Jeffrey C.Y. Chan[1,3], John L. Kelly[3], Abhay S. Pandit[1]*

[1]Department of Mechanical and Biomedical Engineering, National Centre for Biomedical Engineering Science, and Network of Excellence for Functional Biomaterials (NFB), National University of Ireland, Galway, Ireland.

[2]Brunel Institute for Bioengineering, Brunel University, Uxbridge, London, UK

[3]Department of Plastic, Reconstructive and Hand Surgery, University College Hospital, Galway, Ireland

* To whom correspondence should be addressed.

Tel: +353 91492758. E-mail: abhay.pandit@nuigalway.ie.

Running Title: Tailorable *In Vivo* Degradation of CEM

Abstract

This study reports the efficacy of crosslinking on tailoring in vivo biodegradability of cholecyst-derived extracellular matrix (CEM). CEM, two of its N,N-(3-dimethyl aminopropyl)-N'-ethyl carbodiimide (EDC) crosslinked forms EDCxCEM0005 and EDCxCEM0033, and an essentially non-degrading glutaraldehyde-crosslinked control (PeriStrip®) control scaffold were implanted in the subcutaneous tissue in rats. At 7, 28, 63 and 180 days after implantation, rats were killed, implant sites explanted, and processed for histology for qualitative and quantitative evaluation of biodegradation and tissue responses to the implants. Simple quantitative stereological methods provided robust information about the dynamic changes of tissue composition and blood supply at the implant site. Granulation tissue deposition around the scaffolds was complete by 7 days, which matured into dense connective tissue with time. Higher volume of cells and blood vessels was observed at 7 days in the fibrous tissue, which decreased with time. Non-crosslinked CEM showed the phases of 1) granulation tissue deposition within its porous network, 2) resorption of scaffold, 3) concomitant replacement with host tissue and 4) restoration of native adipose tissue composition. The phases were significantly delayed with increasing crosslinking with EDC despite their higher tissue-interacting surface area. GAxBP was impermeable to host tissue infiltration, but appeared to show surface erosion.

Keywords

Cholecyst-derived extracellular matrix, crosslinking, biodegradation, stereology, tissue-implant interactions

1 Introduction

Decellularised extracellular matrices are increasingly being applied clinically because of their biomimetic properties and efficacy as scaffolds for tissue engineering and regeneration.[1] Their efficacy stems from the fact that the decellularisation process removes the antigenic cellular components from natural tissues/organs, while retaining the native collagen structure (3D ECM) and the bioactive molecules such as fibronectin, laminin, growth factors and

cytokines that aid tissue specific host responses when the decellularised ECM is implanted in the body.[2] It is also important to understand that the cocktail of bioactive molecules and native tissue structure depend on their tissue/organ source. For example, the decellularised bone matrix (commercially available as mouldable paste) has type I collagen and bone morphogenic growth factors that aid in bone regeneration.[3] Similarly a basement membrane and/or submucosal derivative, e.g., urinary bladder mucosa (UBM), urinary bladder submucosa (UBS) or small intestinal submucosa (SIS), has the native collagen (type IV) structure of a basement membrane on one side and that of submucosa (type I collagen) on the other.[4] Several such sheets are layered to make the commercial SIS currently available for a variety of soft tissue engineering applications. The compact nature of their native ECM structure makes them impermeable to cellular infiltration, resulting in the scaffold resorption through surface erosion. However, there is also a widespread need for tissue engineering scaffolds that are conducive for cellular infiltration. We identified a new source for intact ECM – the gallbladder/cholecyst, whose serosal layer has a fibro-porous structure that is conducive for cellular infiltration. Earlier, we reported the methods for isolation and decellularisation of the cholecyst-derived ECM (CEM); characterisation of its physico-chemical, mechanical, *in vitro* and *in vivo* biocompatibility; and also demonstrated its efficacy as a scaffold for staple-line reinforcement in an ex-vivo model.[5-10]

Owing to the high surface area and susceptibility to rapid enzymatic degradation of CEM, we envisaged stabilization through carbodiimide (EDC) crosslinking would be required for certain applications, e.g. body wall repair. In our last report, we showed that crosslinking concentration as little as 0.0033 mM of EDC per mg of CEM was sufficient to arrest CEM's susceptibility to collagenase degradation *in vitro*.[6] The objective for the current study was to evaluate the efficacy of crosslinking in prolonging the *in vivo* lifetime of CEM, specifically towards providing mechanical support needed for tissue function. For this purpose, we chose

two EDC crosslinked CEM scaffolds, one slow degrading (EDCxCEM0005) and one that is non-susceptible to collagenase degradation *in vitro* (EDCxCEM0033).

In this study, we report the qualitative and quantitative assessment of scaffold resorption, host tissue deposition and the general tissue responses in a rat subcutaneous implantation model for four test-scaffolds, namely CEM, two of its EDC crosslinked forms and an essentially non-degrading control scaffold - glutaraldehyde crosslinked bovine pericardium (GAxBP). To our knowledge, this study is unique on two counts: the *in vivo* resorption of fibro-porous intact ECM having varying degrees of crosslinking and the quantitation of its dynamics using stereology methods.

CEM has a fibro-porous structure containing macro-pores as well as flexible collagen fibre bundles that cells can displace to aid their rapid infiltration into the bulk of CEM scaffolds.[7, 8] This 3D fibro-porous structure remained intact even after crosslinking with EDC or GA.[6, 7] The typical the fibro-porous morphology of native and EDC crosslinked forms of CEM is illustrated in Fig 1. Unlike SIS or Peristrip, based on the native small intestinal submucosa or the GA crosslinked bovine pericardium respectively, that undergo surface erosion, the biodegradation of CEM follows bulk degradation.[7] The closest analogues for the fibro-porous structure of CEM among man-made tissue engineering scaffolds are electrospun membranes.[11] However, electrospun membranes are limited either by the inertness of synthetic materials (e.g. polyurethane, polylactate-glycolate, polyethylene oxide, or polyethylene glycol) and natural materials (chitosan or spider silk), or by the mechanical weakness of purified natural materials (e.g. collagen, gelatin or polysaccharides). The intact ECM based CEM, in general, is much stronger than the gels or electrospun membranes spun using purified collagen or gelatin.[6, 10] Thus, the fibro-porous structure of CEM in its native and EDC crosslinked forms provides a unique model for *in vivo* bulk degradation among collagen based fibro-porous tissue engineering scaffolds.

Stereology is a science based on the principles of geometry and statistics that provides simple, powerful, fast, accurate, objective, reproducible and verifiable methods to acquire 3D quantitative information from 2D slices.[12-16] Its use in quantitation of tissue-implant interactions outside our group is still very limited.[17, 18] We consistently utilize the stereology approach to quantitate tissue-implant interactions.[7, 11, 12, 19-22] In this study, we utilized point count methods of stereology employing grids of known dimensions to estimate volume per unit volume (V_v), surface area per unit volume (S_v), length per unit volume (L_v) and radial diffusion distance (R_{diff}) between tubular structures (blood vessels). Such quantitative information served as a model to describe the dynamic changes in tissue responses, blood supply, scaffold resorption, as well as host tissue deposition and maturation at the implant site.

2 Materials and Methods

All reagents unless otherwise stated were purchased from Sigma Ireland Ltd. Dublin, Ireland. Fresh cholecysts of market weight farm-reared pigs (Sean Duffy Exports Ltd., Gort, Ireland) were transported to the laboratory on ice and processed within six hours of killing the pigs.

2.1 Isolation of CEM

CEM was isolated from porcine cholecysts and decellularised with peracetic acid solution in ethanol according to the protocol reported earlier[8] Briefly, excess liver tissue was removed and bile fluid drained. The neck and fundus of the cholecyst were trimmed, followed by a longitudinal incision to obtain a flat sheet of tissue. The mucosa, lamina propria and muscularis layers were peeled from the luminal side, followed by a similar process to remove the serosal mesothelium and its underlying connective tissue from the abluminal side. Any residual elements were removed by mechanical delamination on both sides. A solution of 0.15% peracetic acid in 4.8% ethanol in deionized water was used to decellularise the sheet of tissue for 30 min. Following decellularisation, the samples were washed thoroughly in phosphate-buffered saline (PBS) and distilled water. The resulting matrix was directly used for carbodiimide cross-

linking. The non-cross-linked CEM samples (controls) were freeze dried (Virtis Advantage Freeze Dryer, Gardiner, NY, USA) and stored in vacuum desiccators until further use.

2.2 Cross-linking of CEM with Carbodiimide

Fresh decellularised CEM samples were cross-linked with N,N-(3-dimethyl aminopropyl)-N'-ethyl carbodiimide (EDC) and N-hydroxysuccinimide (NHS) in 2-morpholino-ethanesulfonic acid (MES) buffer (pH 5.3, 0.05 M) for 4 h at 37ºC. A 1:1 EDC to NHS molar ratio was used for all cross-linking. For this study, two crosslinking concentrations namely 0.0005 and 0.0033 mmol of EDC per mg of CEM were used.[6] Following crosslinking, the samples were washed thoroughly with PBS and distilled water, and freeze dried. The samples were designated as EDCxCEM0005 and EDCxCEM0033, the numerical suffix indicating the initial feed cross-linking concentration of EDC per mg of CEM. The non-cross-linked CEM is designated as CEM.

2.3 Implants Selection for Subcutaneous Implantation

To assess our ability to tailor *in vivo* degradation of CEM, four implant types, namely CEM, EDCxCEM0005, EDCxCEM0033 and glutaraldehyde-crosslinked bovine pericardium (GAxBP) were chosen. GAxBP, the control scaffold, was a commercial staple-line reinforcement product named Peri-Strips® (Synovis Surgical Innovations, Minnesota, USA), which is a relatively inert decellularised ECM-based scaffold. In our earlier study, we showed that the collagenase susceptibility of CEM can be tailored through EDC crosslinking[6] A crosslinking concentration of 0.0005 mmol EDC per mg CEM caused about 80% decrease in weight following 48 h exposure to collagenase, compared to about 90% decrease observed with CEM. The concentration of 0.0033 mmol, on the other hand, was the minimum concentration needed to completely resist collagenase degradation (close to 0% decrease in weight). CEM was shown to lose mechanical integrity within 28 days and to be completely resorbed within 63 days[7]. The crosslinked CEM samples - EDCxCEM0005 and EDCxCEM0033 - were anticipated to degrade much slower *in vivo* compared to CEM.

2.4 Implantation in rats

Six week old Sprague Dawley rats (Harlan UK Ltd., Oxon, UK) weighing between 150 and 200 g were housed in the experimental animal facility at National Centre for Biomedical Engineering Science, Galway. All animal procedures had ethical approval from Institutional Animal Ethics Committee of the National University of Ireland - Galway, and the studies were also covered under the license issued by Department of Health and Family Welfare, Ireland. The rats were acclimatized to local environment for 1 week prior to surgery.

The rats were anaesthetized with ketamine (100 mg/kg) and xylazine (5 mg/kg) and the dorsal skin shaved and disinfected. Along the dorsal midline, three 15 mm longitudinal incisions were made, about 30 mm apart. At each incision, two lateral subcutaneous pockets were made. In each pocket one 10 x 10 mm scaffold was immobilized at the subcutaneous level using a non-degradable Ethicon™ 4-0 Prolene® (Johnson & Johnson Ireland Ltd., Dublin, Ireland) about 10 mm away from the incision. The incisions were closed using a degradable Ethicon™ 4-0 Vicryl® (Johnson & Johnson Ireland Ltd., Dublin, Ireland). The rats were given standard pellet diet and fresh water. The implant sites were physically observed at regular intervals.

A total of sixteen rats were divided into four groups of four rats each. Each rat received six implants. The positions of the implants were randomised such that each implant type occurs once at each of the six positions on the dorsum of the rats for each time-point. The animals were killed at 7, 28, 63 and 180 days and implant sites excised for histology and fixed in 4% neutral buffered formalin.

2.5 Histopathology

Formalin fixed tissues were dehydrated through graded ethyl alcohol solutions (50%, 75%, 95%, and 100%), cleared with xylene and embedded in paraffin. The processing of the tissues was done in automatic tissue processor (Leica ASP 300, Leica Microsystems, Nussloch, Germany). Five-micrometer thick paraffin sections were stained with hematoxylin and eosin (H&E), and Masson's trichrome (MT). H&E and MT stains were used to evaluate the general

histomorphology and quantitative stereological analysis at the implant sites. The stained sections were observed under light microscope and digital images captured for stereological analysis (BX51 microscope, DP-70 digital camera, Olympus Europe, Hamburg, Germany).

2.6 Quantitative stereological analysis

The different stereological methods utilized for the quantitation of tissue response and degradation parameters in this study, were based on the practical examples reported by Garcia et al and Burugapalli et al.[7, 12] The stereological approach is based on sampling and sampling needs to be isotropic.[12, 13] Since cutaneous tissue is an anisotropic layered structure, its stratified nature required the use of vertical uniform random sampling method to obtain isotropy in the vertical sections.[13, 16, 23, 24] Six non-overlapping random fields of view per section per each stereological parameter; three sections per treatment; and six treatments per test scaffold per time-point, were used for adequate sampling.[12] The probes/test systems (counting frames, grids etc.) and other image analysis tools provided by an image analysis software (Image Pro® Plus, Media Cybernetics, UK) were used to enable point counts for the stereological estimations.

The stereological parameters and probes used for the quantification on histology sections are summarized in Table 1. For stereological analysis the implant site was divided into two regions, namely, the implant area and the fibrous tissue surrounding the implant. Stereological volume fraction (V_v) estimations of collagen, nuclei, cytoplasm and blood vessels were used for the evaluation of tissue composition and scaffold degradation, while surface density (S_v), length density (L_v) and radius of diffusion (R_{diff}) estimations were used to evaluate the nature and distribution of blood vasculature in both implant area and its surrounding fibrous tissue.

2.7 Statistical analysis

Statistical analyses were carried out using statistical software (SPSS v.18). Statistical variances between groups were determined by one way analysis of variance (ANOVA). Tukey's honestly significant difference test was used for *post hoc* evaluation of differences between

groups. A p value of <0.05 was considered to be statistically significant. All data represented are expressed as mean ± standard error (SE) of mean.

3. Results

All rats survived the surgery and the study period. Skin at the implant sites did not show any signs of ulceration, infection or wound dehiscence. At the end of the study period, the rats were killed, the implant sites examined for residual implants and then excised along with surrounding skin for histology assessments. Where the implants were completely resorbed, the implant sites were identified by locating the non-degradable Prolene sutures used to secure the implant at the time of implantation.

Morphology examination of the explanted tissues showed that the implant sites had varying amount of remaining implants visible. Non-crosslinked CEM showed no visible remaining implants at 63 and 180 days. Remains of the implants EDCxCEM0005 and EDCxCEM0033 were seen at 63 and 180 days. The positive control GAxBP implants appeared intact in size and stiffness even after 180 days of implantation. All implants were integrated into the subcutaneous tissue, but did not appear to be encapsulated with thick fibrous capsules.

3.1 Qualitative Histopathology

Histologically all scaffolds were integrated in the fibrous connective tissue (wherein fat cells accumulate with ageing) sandwiched between the subcutaneous smooth muscle and the underlying skeletal muscle tissue of the body wall. The regions of interest at the implant site are the implanted scaffold and its immediately surrounding fibrous tissue. The subcutaneous muscle did not show any obvious changes in histological structure, indicating that the foreign body reactions are restricted closer to the surface of the implanted scaffolds.

3.1.1 Fibrous Tissue Surrounding Implant Area

Figure 2 shows the histological structure of the fibrous tissue between the implant surface and subcutaneous smooth muscle for the four implant types as a function of time. By 7 days distinct fibrous connective tissue formed around all test-scaffolds. The FT was composed of

loose connective tissue rich in collagen and blood vessels. The collagen fibre bundles and fibroblasts within the FT were orientated parallel to the long axis of the subcutaneous muscle and surface of the implant area.

The general trends for histological changes of composition of FT around all the test scaffolds were similar (Fig 2). The collagen bundle thickness and packing increased, while the density of cells and blood vessels decreased with time. Any inflammatory cells present were localised closer to the blood vessels or at the interface between the implant surface and host tissue. No neutrophils, eosinophils, mast cells, basophils or plasma cells were observed indicating the absence of acute inflammation and allergic reactions. The inflammatory cells were mainly macrophages and lymphocytes, indicating that the body is actively degrading and resorbing the implanted test scaffolds. At 7 days, no fibrocytes (mature and inactive fibroblasts, with hardly any cytoplasm) were seen, but their numbers increased as the FT matured at 63 and 180 days.

Typically, at all time-points, the fibrous tissue for all CEM based scaffolds had uniform collagen bundle structure across its cross-section from the surface of implant to the subcutaneous muscle, indicating minimal or no mechanical stress induced by the implanted scaffold. However for GAxBP, at their interface with host tissue, a highly aligned and dense fibrous tissue formed, the thickness of which appeared to increase with time. The blood vessels in the FT around all CEM based scaffolds were oval in shape, similar to that of native connective tissue adjacent to the subcutaneous smooth muscle. On the other hand, the blood vessels in the FT for GAxBP scaffolds were spindle shaped, with tapered ends, which could also be an indicator for the stiffer GAxBP that doesn't allow host tissue infiltration into its bulk.

In addition, the host cells and collagen at the scaffold-tissue interface were continuous with the host tissue infiltrating in to the CEM scaffolds. On the other hand, cells failing to infiltrate the bulk of GAxBP scaffold accumulated at the tissue-scaffold interface. Typically,

there was a 1 to 10 cells thick layer on the immediate surface of GAxBP, the cells mainly composed of macrophages and lymphocytes.

3.1.2 Implant area

The typical histological structure of implant area for all implant types at all time-points is shown in Figure 3. The typical degradation profile ending in complete remodelling of tissue is evident from the implant area of non-crosslinked CEM. At 7 days, the whole of the implant was infiltrated with the host's cells and blood vessels, while the implant collagen (in darker blue coloured and dense bundles) was intact. The cells were mononuclear, typically consisting of fibroblasts, macrophages, and lymphocytes, with occasional plasma cells, and no neutrophils, eosinophils, basophils or mast cells. At 28 days the implant collagen is mostly replaced by new collagen (lighter blue and loose packing), and cells predominantly macrophages, fibroblasts and lymphocytes. By 63 days, the implant collagen appeared to be completely resorbed and the presence of fat cells, fibroblasts, and mononuclear cells is indicative that the implant site is remodelled to the native subcutaneous tissue structure. The remodelled tissue appears to have matured (having denser collagen) and truly representing the native subcutaneous adipose connective tissue at 180 days.

The histological structure of implant area for EDCxCEM samples was indicative of the stages of degradation, similar to that observed with non-crosslinked CEM, including the infiltrating cell composition. However, the crosslinking only delayed the degradation rate for EDCxCEM similar to that observed *in vitro* (collagenase degradation), except that the *in vivo* degradation is significantly prolonged. At 7 days both the EDCxCEM implants were completely infiltrated with host cells and implant collagen intact, except that the collagen bundles were thicker than that of CEM, as a result of crosslinking. Most of the implant collagen was intact at 28 days, with little new collagen deposition. Active resorption of implant collagen accompanied by its replacement with new collagen having an organised connective tissue structure with occasional fat cells is evident for EDCxCEM0005 at 63 days which was still the case at 180

days. However this phase appears to have just started for EDCxCEM0033 at 63 days and the tissue was better organised and remodelling by 180 days. The positive control GAxBP, on the other hand, did not show any signs of bulk degradation even after 180 days of implantation. The implant collagen remained intact, with occasional host mononuclear cells especially at the edges of the scaffold, where the pores of the scaffold are accessible to the surrounding host tissue. However, degradation in case of GAxBP could be occurring through surface erosion as indicated by the accumulation of dense fibrous tissue at the tissue implant interface.

3.2 Quantitative Histopathology

Chronological changes in the histological structure of the fibrous tissue surrounding the implant as well as the implant area were quantified using stereology estimations based on point counts. V_v of collagen, nuclei, cytoplasm and blood vessels were used to monitor dynamic changes of tissue composition, while S_v, L_v and R_{diff} for that of blood vasculature.

3.2.1 Fibrous Tissue Surrounding Implant Area

Linear regression of the V_v data (Fig 4a-d) as a function time indicates the general trends for changes in tissue composition of the FT surrounding scaffolds revealed an increase of V_v of collagen with concomitant decrease in V_v of nuclei, cytoplasm and blood vessels (with the exception of V_v of cytoplasm for GAxBP). A closer look at the quantitative stereology estimations of V_v of tissue components namely collagen, nuclei, cytoplasm and blood vessels, shown in Fig 4a-d, reflect the nature of host responses to the different test scaffolds having varying rates of biodegradability and permeability to host tissue infiltration.

V_v of collagen increased near linearly from day 7 to day 63 for all test scaffolds, which is indicative of the maturation of the deposited loose granulation tissue into denser fibrous connective tissue (Fig 4a). In general, the V_v of collagen at 7 days is significantly different from that at 63 and 180 days. After 63 days, a steady state for V_v of collagen appears to have been attained, indicating a steady state for host tissue-scaffold interactions for all scaffolds except CEM. A further increase in collagen content was observed for FT around the implant area for

CEM, which, in conjunction with the qualitative observation (Fig 2 and 3) is suggestive of the resolution of host response following complete degradation and resorption of CEM and its replacement with adipose connective tissue.

The V_v of nuclei in fibrous tissue surrounding all test scaffolds decreased with time (Fig 4b). The decrease was statistically significant between 7 and 180 days after implantation for all scaffolds. In addition, it was interesting that the decrease was linear for CEM from 7 to 63 days, which could reflect the gradual/constant rate of removal of the bulk of CEM and its replacement with native subcutaneous adipose connective tissue as reflected in the qualitative observations (Fig 3).

The changes in the V_v of cytoplasm in the fibrous tissue surrounding the different test scaffolds are shown in Fig 4c. Only for CEM V_v of cytoplasm in fibrous tissue showed a linear decrease from 7 to 180 days. The decrease was significant between 7 and 180 days for CEM and EDCxCEM0005. A steady-state appears to have been reached for EDCxCEM0005 and GAxBP from days 28 to 180. There was no clear trend observed for EDCxCEM0033.

The blood vessel content in fibrous tissue surrounding all test scaffolds, as reflected by their V_v, in general, decreased with time, but the differences in the stereology estimations were statistically insignificant within and between the test-scaffolds (Fig 3d). Prominent presence of blood vessels in FT around all implant types is observed (Fig 5a-c). Stereology analysis of surface density (S_v), length density (L_v) and inter-blood vessel radial-diffusion (R_{diff}) distance showed distinct trends indicative of the degradation profiles of the respective implant types. Highest S_v, L_v and corresponding lowest R_{diff} was observed at 7 days for all implants. The higher blood vessel content was correlating with the corresponding cell content for the implants. The higher the number of cells the higher is the cell metabolism, and thus higher the blood supply. As the inflammation subsided, the blood vessel content showed a decreasing trend. The decrease was significant for the fast degrading CEM and the slow degrading GAxBP. However, the

decrease in blood vessel content was not statistically significant for both the slow degrading crosslinked CEM implants.

3.2.2 Implant area

The influence of porosity and biodegradability of the test-scaffolds on V_v of collagen, within the implant area (scaffold bulk) is shown in Fig 6a. About 96% of the bulk of GAxBP was collagen at all time-points, which is attributed to its practically non-porous structure and hence non-susceptibility to bulk degradation. However, the porous structure of the CEM based scaffolds, showed varying V_v of collagen depending on their degrees of crosslinking. Typically, the porous network is initially filled by infiltrating host cells, which later deposit host collagen that gradually fills the pores and matures with time, thus resulting in the increase in V_v of collagen within the implant area. The increase in V_v of collagen continued to the end of the study period of 180 days for EDCxCEM0005 and EDCxCEM0033, but was only until 28 days for CEM. The lower V_v of collagen ($p<0.05$) for CEM at 63 and 180 days is due to the replacement of the resorbed CEM scaffold with adipose connective tissue (a significant volume of which is the fat cells). The V_v of collagen within EDCxCEM0005, with a slight crosslinking was similar to that observed for CEM at 7 and 28 days, while that of EDCxCEM0033 is much less ($p<0.05$). This can be attributed to a stiffer EDCxCEM0033 that retains the integrity of its open porous network due to high degree of crosslinking

The effect of stiffer network structure of EDCxCEM0033 and its open porous structure is also reflected by the higher V_v of nuclei at days 7 to 63, especially at day 7 ($p<0.05$), compared to that of CEM and EDCxCEM0005 (Fig 6b). About 2% of GAxBP implant area consisted of V_v of nuclei, which could be of cells that enter the implant area through the cut ends of the highly crosslinked GAxBP (Fig 5b). No change in the V_v of collagen, nuclei, cytoplasm, or blood vessels across all time-points for GAxBP (Fig 6a-c) clearly indicates limited effect of host reactions in the implant area of GAxBP.

The dynamics of V_v of cytoplasm in the implant areas of the different test-scaffolds, shown in Fig 6c, are indicative of the nature of cells infiltrating the scaffolds. The higher V_v of cytoplasm at all-time points for CEM-based scaffolds, with the exception of CEM at 63 and 180 days is indicative of macrophages (having high cytoplasm content) predominating the cells infiltrating the scaffolds. Statistically higher cytoplasm content for EDCxCEM0033 at 7 days compared to CEM and EDCxCEM0005 again correlate with the infiltration of larger numbers of cells (esp. macrophages) into the open porous network structure of EDCxCEM0033. The higher V_v of cytoplasm (25 to 30%) for CEM at 63 and 180 days ($p>0.05$) is due to the fat cells that accumulated in the subcutaneous tissue, replacing CEM, that resulted in a lower V_v of collagen in this tissue.

The blood vessels infiltrating the implant area were reflective of the cellular content and activity within the scaffold (Fig 7). The larger number of cells within EDCxCEM0033 at day 7 as reflected with high V_v of nuclei and cytoplasm correlated with statistically higher V_v of blood vessels compared to that observed with EDCxCEM0005 and GAxBP. The higher V_v of blood vessels for CEM at 63 and 180 days could be indicative of active deposition of fat in the subcutaneous adipose connective tissue. Essentially, blood vessels failed to infiltrate into the implant area of GAxBP as reflected by their V_v close to 0%. The general decrease in the V_v of blood vessels for EDCxCEM scaffolds from days 7 to 180 is indicative of a general decline in cellular content and activity within the implant area with time. The trends in S_v, L_v and R_{diff} of blood vessels in implant areas in general appear to be similar to that observed with V_v of nuclei indicating that the blood vessel content is proportional to the metabolically active cells present in the tissue (Fig 7a-c).

4 Discussion

Based on the *in vitro* collagenase degradation profiles of the different EDCxCEM samples (as reported in our earlier study[6]), EDCxCEM0005 and EDCxCEM0033 were chosen as the slow degrading (80% weight loss in 48h) and collagenase non-susceptible (0% weight loss

in 48h) scaffolds respectively, to study our ability to tailor *in vivo* biodegradation rates of CEM using crosslinking. Commercial GAxBP (PeriStrip®) was used as the non-degradable decellularised ECM control scaffold. The four test-scaffold types were implanted in the subcutaneous tissue of rats to evaluate their interaction with host tissue and *in vivo* biodegradability using qualitative and quantitative histological assessments.

Tissue injury due to implantation invariably introduces fibrin based provisional matrix around the implant, which is eventually replaced by granulation (fibrous) tissue.[25] This study showed that the granulation tissue formation is complete by 7 days around all scaffolds-types tested. About 55 to 65% of the volume of this tissue was collagen (Fig 4a), and histologically, it was loose connective tissue containing large number of fibroblasts (Fig 2). The lower V_v of collagen for all test-scaffolds at 7 days can also be attributed to the presence of large number of mononuclear cells other than fibroblasts, the volume of which reflected on the degree of specific scaffold-tissue interactions. By 63 days after implantation, the V_v of collagen in the fibrous tissue surrounding all test-scaffolds increased to about 80% (Fig 4a), essentially indicating the slow process of maturation of the fibrous tissue, as reflected by the appearance and increase in the number of fibrocytes (mature fibroblasts) and increase in thickness and density of the collagen bundles (Fig 2). Between 63 and 180 days, the V_v of collagen in the fibrous tissue surrounding EDCxCEM0005, EDCxCEM0033 and GAxBP remained stable. However, for CEM it further increased close to 90% by 180 days (Fig 4a). This difference of about 10% in the V_v of collagen between CEM and the rest of the scaffolds may be the difference between the complete removal and the presence of scaffold collagen respectively. Histologically, higher numbers of macrophages and lymphocytes were observed in the fibrous tissue surrounding EDCxCEM0005, EDCxCEM0033 and GAxBP, which is indicative of the persistence of tissue responses to residual scaffolds at the implant site. The higher number of cells in the fibrous tissue at 180 days for scaffolds other than CEM was also confirmed by the combined higher V_v of nuclei and

cytoplasm (Fig 4b&c, 14 to 19% compared to 10% for CEM). It is also important to note that these cells were concentrated closer to blood vessels.

The dynamic changes in the V_v of nuclei and cytoplasm, both individually and combined, were suggestive of the nature of scaffold-tissue interactions. V_v of nuclei in the fibrous tissue surrounding the scaffolds were highest for CEM and GAxBP (about 20%), but the combined V_v of nuclei and cytoplasm was highest for CEM and EDCxCEM0033 (about 32%). Thus, in terms of number of cells, fibrous tissue around CEM and GAxBP had the highest, which can be attributed to the contrasting natures of the two scaffold types. The former, has large number of cells (primarily macrophages as indicated by the higher V_v of cytoplasm) that are actively removing the scaffold from the site of implantation, while the latter being impermeable to cells, resulting in accumulation of all cells at its surface and the surrounding fibrous tissue. Furthermore, the low V_v of cytoplasm for GAxBP is indicative of a lower number of macrophages and a larger population of lymphocytes, which could be associated with the combined effect of its non-susceptibility to enzymatic degradation due to glutaraldehyde crosslinking and smaller scaffold-tissue interface area. Considering the non-susceptibility of EDCxCEM0033 to collagenase degradation *in vitro*, we can also expect it to show cellular responses similar to that observed with GAxBP. On the contrary, a large population of macrophages was seen in the fibrous tissue surrounding EDCxCEM0033. The macrophage population with higher cytoplasm content than that observed with CEM could be associated with the removal of provisional matrix and cell debris deposited within the porous network of EDCxCEM0033 rather than the removal of the scaffold (Fig 3 & 5). On the other hand, light crosslinking in EDCxCEM0005 lowered the number of cells (primarily macrophages) recruited to remove the slow degrading scaffold. The constant V_v of cytoplasm (about 7%) in the fibrous tissue surrounding EDCxCEM0005 from days 28 to 180 is suggestive of a slow and steady resorption of the underlying scaffold by macrophages.

The qualitative and quantitative evaluation of tissue composition in the implant area further revealed the effects of crosslinking on the *in vivo* fate of the different test-scaffolds. Non-crosslinked CEM provided a good example for stages of complete resorption of a tissue engineering scaffold and restoration of the implant site to its native tissue configuration (Fig 3). At 7 days the implant was intact and completely infiltrated with host cells. The implant area for CEM consisted of 74% collagen by volume, 24% cells (V_v of nuclei + cytoplasm) and 2% blood vessels. By 28 days the most of the implant was resorbed and replaced by a well organised new host collagen deposition. Complete resorption and restoration to native host subcutaneous adipose tissue configuration was achieved by 63 days, which is even more prominent at 180 days after implantation.

GAxBP, on the other hand, is nearly 100% crosslinked commercial product intended for long-term implantation. It served as a positive control for non-degrading/very slow degrading scaffold. However, its decellularised dense native collagen tissue and crosslinking rendered the implant non-porous and hence impermeable to host cell infiltration. As a result, it was only susceptible to surface degradation (Fig 2 & 3). Compared to the porous CEM based scaffolds, the surface area exposed for degradation for the non-porous GAxBP is very small leading to a very slow *in vivo* resorption rate. The degradation rate was so slow that even after 180 days, the GAxBP scaffolds retained their stiffness and integrity. SIS, a commercial decellularised scaffold is reported to be non-crosslinked. However, its native collagen organisation is such that it is non-porous and does not allow infiltration of host cells in to the scaffold. Yet, an 8 layered such scaffold is reported to degrade completely within 90 to 180 days and assist regeneration of native tissue at the site of implantation.[26] Our study demonstrated that even a low degree of crosslinking can significantly prolong the *in vivo* life of the ECM based scaffolds and the degree of crosslinking can be used to tune the *in vivo* life of a regenerative scaffold to suit desired applications.

Crosslinking essentially delayed the different stages of degradation observed with non-crosslinked CEM (Fig 3). All CEM based scaffolds were completely infiltrated with host cells by 7 days, but the deposition of host collagen within their porous network was significantly delayed for EDCxCEM0033. The decrease in the content of sites for cell attachment, the stiffer collagen bundles and the open porous network due to crosslinking can result in the deposition of a larger volume of provisional matrix that requires removal by macrophages (as indicated by the significantly large V_v of nuclei and cytoplasm). Thus, the nearly 100% crosslinking of the collagen bundles of CEM by EDC could be responsible for the significant delay in the deposition of the host collagen within the fibro-porous network of EDCxCEM0033. EDCxCEM0005, on the other hand, had V_v of collagen within its matrix similar to that observed for non-crosslinked CEM at 7 and 28 days. However, its slight crosslinking with EDC ensured stability, such that the collagen bundles of CEM are present even after 180 days after of implantation. The appearance of fat cells within the network of EDCxCEM0005 at 63 days indicates that the implant site entered a remodelling phase. Contrary to that observed with the CEM based scaffolds, GAxBP was impermeable to host tissue infiltration and its tissue composition remained constant till the end of the study period of 180 days.

In addition, quantitative stereology assessments also provided insights into the dynamics of blood supply at the site of implantation. High blood vessel surface area and length per unit volume, and low inter-vessel radial diffusion distance is observed in FT compared to that in the implant area. Further, higher the volume fraction of cells in the tissue, the higher was the observed blood vessel content, reiterating that blood vessel growth or regression is a dynamic process working as per need. It is interesting that the blood vessel content, in terms of V_v, S_v, L_v and R_{diff}, is similar between the fibrous tissue and the remodelled adipose connective tissue that replaced CEM, which could be an indicator for complete resorption of the tissue engineering scaffolds and restoration of the native tissue composition.

5. Conclusion

The fibro-porous native CEM, which degrades completely within one hour of immersion in collagenase solution *in vitro*,[6] took about 2 months to get completely absorbed from the subcutaneous site of implantation in rats. However, residual collagen of the EDCxCEM0005 scaffold (crosslinked with 5mM of EDC per mg of CEM, 80% of whose weight is lost within one hour of immersion in collagenase solution *in vitro*) was very much present even after 6 months after implantation. Essentially, the stages of CEM's *in vivo* degradation and removal from the site of subcutaneous implantation that are complete within 2 months were significantly delayed with increasing EDC crosslinking. Unlike CEM based fibro-porous scaffolds, GAxBP that was essentially impermeable to host cell infiltration and collagen deposition was only susceptible to surface erosion and most of its bulk was intact in structure and form even after 6 months of implantation. Stereological quantitation revealed a correlation between cell numbers and blood vascular supply to the tissue, and in general helped better understand and describe the dynamics of tissue composition at the implant site. To conclude, even a tiny degree of crosslinking can significantly prolong the rate of *in vivo* degradation and removal of CEM, a fibro-porous decellularised intact ECM.

Acknowledgements

This work was funded by Enterprise Ireland – Technology Development grant.

References

[1] S. F. Badylak, D. O. Freytes, T. W. Gilbert, *Acta Biomaterialia* **2009,** *5*, 1.

[2] T. W. Gilbert, T. L. Sellaro, S. F. Badylak, *Biomaterials* **2006,** *27*, 3675.

[3] I. Marcos-Campos, D. Marolt, P. Petridis, S. Bhumiratana, D. Schmidt, G. Vunjak-Novakovic, *Biomaterials* **2012,** *33*, 8329.

[4] C. A. Barnes, J. Brison, R. Michel, B. N. Brown, D. G. Castner, S. F. Badylak, B. D. Ratner, *Biomaterials* **2011,** *32*, 137.

[5] K. Burugapalli, J. C. Y. Chan, J. L. Kelly, A. Pandit, *Obes Surg* **2008,** *18*, 1418.

[6] K. Burugapalli, J. C. Y. Chan, H. Naik, J. L. Kelly, A. Pandit, *J Biomater Sci Polym Ed* **2009,** *20*, 1049.

[7] K. Burugapalli, A. Pandit, *Biomacromolecules* **2007,** *8*, 3439.

[8] K. Burugapalli, A. Thapasimuttu, J. C. Y. Chan, L. Yao, S. Brody, J. L. Kelly, A. Pandit, *Biomacromolecules* **2007,** *8*, 928-936.

[9] S. Brody, J. McMahon, L. Yao, M. O'Brien, P. Dockery, A. Pandit, *Biomaterials* **2007,** *28*, 1461.

[10] J. C. Coburn, S. Brody, K. L. Billiar, A. Pandit, *J. Biomed. Mat. Res.* **2007,** *81A*, 250.

[11] J. A. Henry, K. Burugapalli, P. Neuenschwander, A. Pandit, *Acta Biomaterialia* **2009,** *5*, 29.

[12] Y. Garcia, A. Breen, K. Burugapalli, P. Dockery, A. Pandit, *Biomaterials* **2007,** *28*, 175.

[13] T. M. Mayhew, *Exp. Physiol.* **1991,** *76*, 639.

[14] L. M. Cruz-Orive, E. R. Weibel, *Am. J. Physiol.* **1990,** *258*, L148.

[15] J. C. Russ, R. T. Dehoff, "Classical stereology measures". in *Practical stereology*, 2nd edition, Plenum Press, New York **1999,** p. 39.

[16] C. A. Mandarim-De-Lacerda, *An. Acad. Bras. Ciênc.* **2003,** *75*, 469.

[17] J. E. Sanders, S.E. Lamont, S. B. Mitchell, S. G. Malcolm, *J. Biomed. Mater. Res.* **2005,** *72A*, 335.

[18] U. Klinge, V. Schumpelick, B. Klosterhalfen, *Biomaterials* **2001,** *22*, 1415.

[19] G. Damodaran, W. H. C. Tiong, R. Collighan, M. Griffin, H. Navsaria, A. Pandit, *J. Biomed. Mater. Res. A* **2013**.

[20] Y. Garcia, B. Wilkins, R. J. Collighan, M. Griffin, A. Pandit, *Biomaterials* **2008,** *29*, 857.

[21] A. M. Breen, P. Dockery, T. O'Brien, A. S. Pandit, *Biomaterials* **2008,** *29*, 3143.

[22] A. Breen, P. Dockery, T. O'Brien, A. Pandit, *J. Biomed. Mater. Res.* **2009,** *89A*, 876.

[23] U. Hahn, A. Micheletti, R. Pohlink, D. Stoyan, H. Wendrock, *J. Microsc.* **1999,** *195*, 113.

[24] C. V. Howard, M. G. Reed, “Unbiased stereology: three-dimensional measurement in microscopy”, in *Advanced methods*, 2nd edition, edited by C. Jones, Garland Science/BIOS Scientific Publishers, Abingdon, Oxon, UK **2005**.

[25] J. C. Y. Chan, K. Burugapalli, J. L. Kelly, A. Pandit, “Influence of Clinical Application on Bioresorbability: Host Response”, in *Degradation Rate of Bioresorbable Materials: Prediction and Evaluation*, edited by F. Buchanan, Woodhead Publishing Ltd., Cambridge, England **2008**, p. 267.

[26] S. F. Badylak, *Transpl. Immunol.* **2004,** *12*, 367.

Table 1: Stereological methods used in this study for the evaluation of tissue response and degradation parameters at subcutaneous implantation site.

Stereology Parameter	**Probe: Orientation and Dimensions**	**Equation**
Volume Fraction/Density (V_v)	Grid made of 30 x 30 µm squares, with a total of 88 intersection; 400x mag.	$V_v = \frac{P_P}{P_T}$
Surface Density (S_v)	Cycliod grid; cycloid arc height - 10 µm; 10 arcs/line; 6 lines/grid; 400x mag.; Oriented perpendicular to vertical axis of VUR section	$S_v = 2 \times \frac{I}{L_T}$
Length Density (L_v)	Cycliod grid; cycloid arc height - 10 µm; 8 arcs/line; 8 lines/grid; 400x mag.; Oriented parallel to vertical axis of VUR section	$L_v = \frac{\left(2 \times {}^{I}/_{L_T}\right)}{T_S}$
Radius of Diffusion (R_{diff})	Same as that for L_v measurements	$R_{diff} = \frac{1}{\sqrt{\pi \times L_v}}$

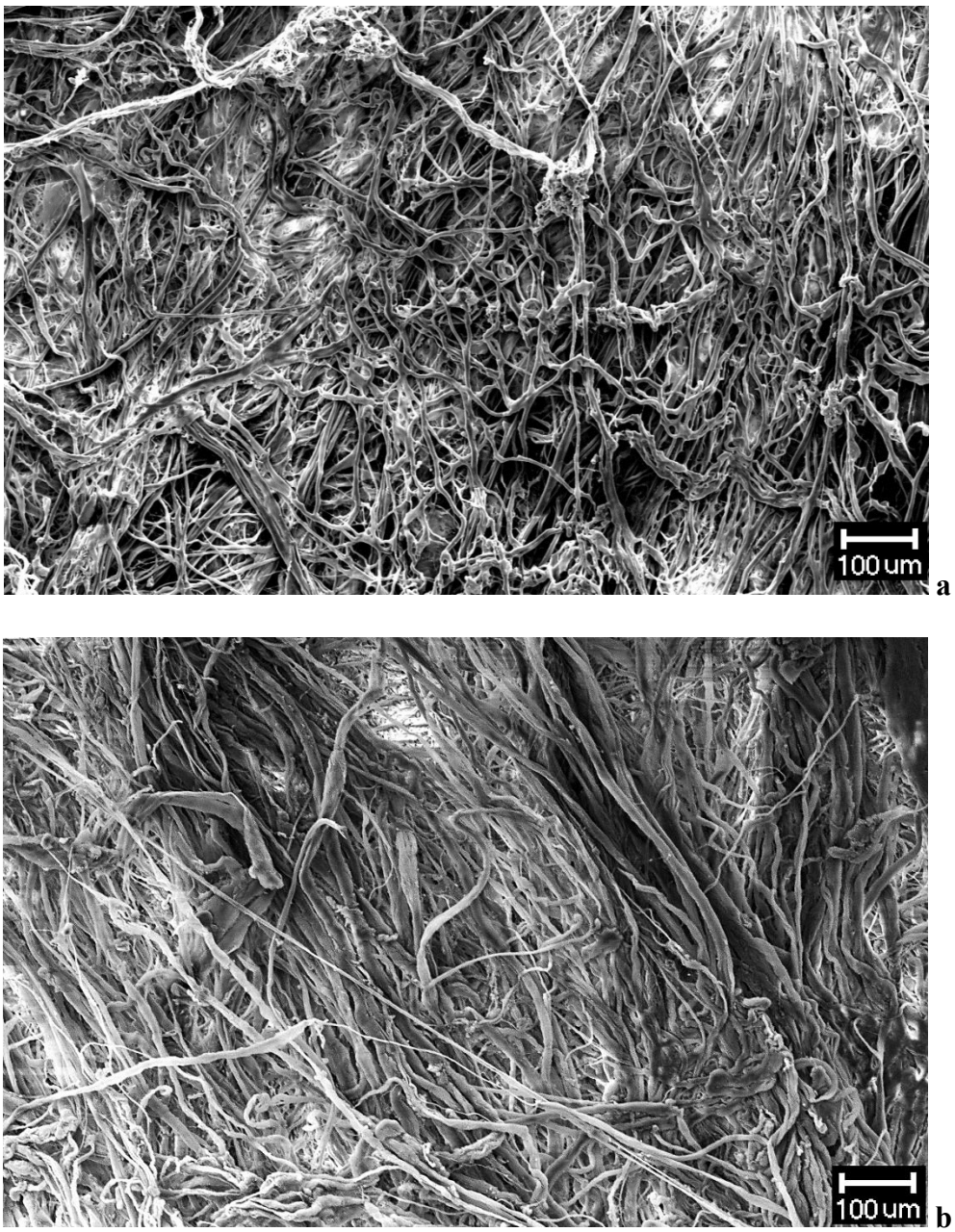

Figure 1: Scanning electron micrographs showing morphology of the freeze-dried (a) native and (b) EDC crosslinked forms of the cholecyst-derived extracellular matrix.

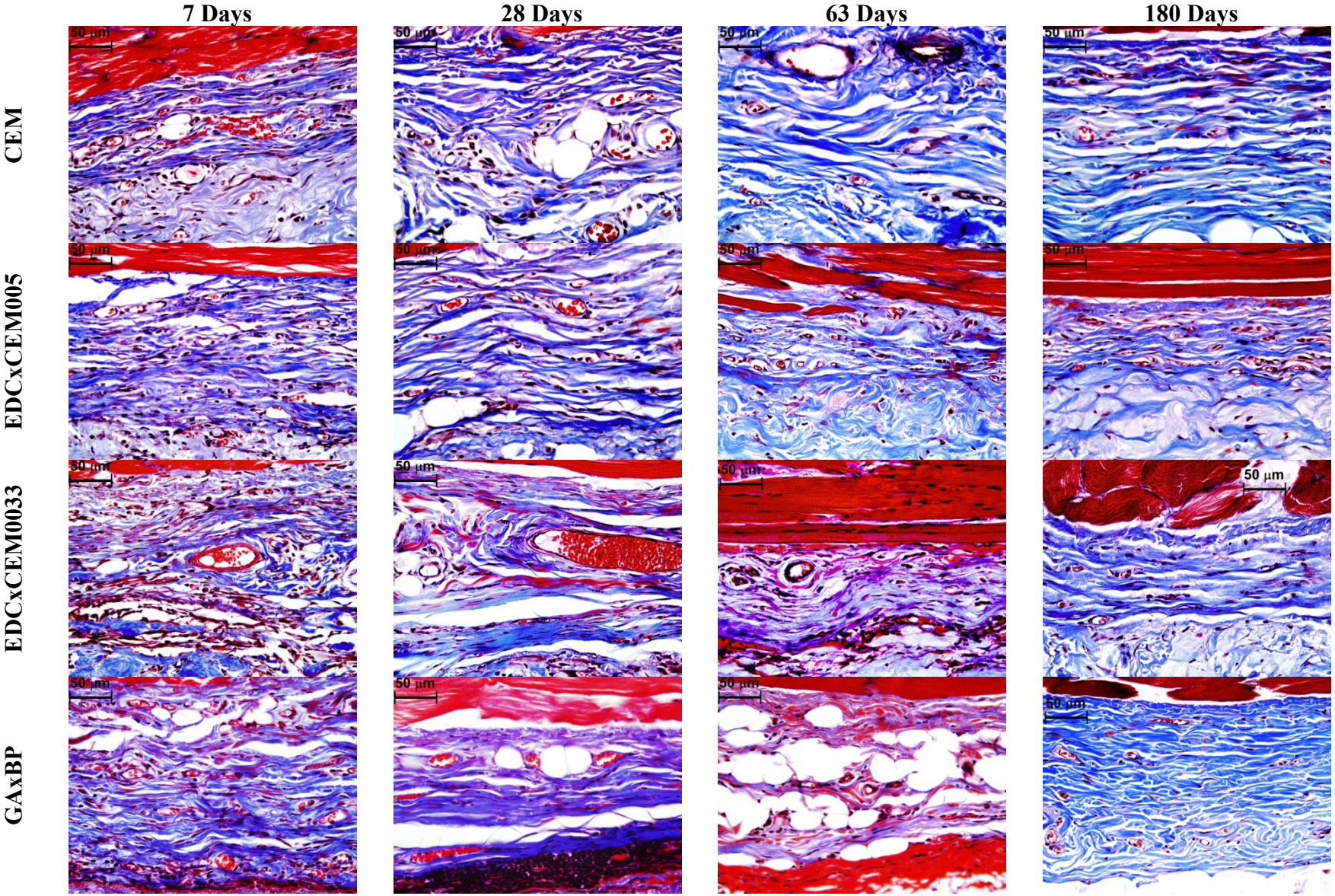

Figure 2: Masson's Trichrome stained histology sections showing the fibrous tissue around the different implants as a function of time.

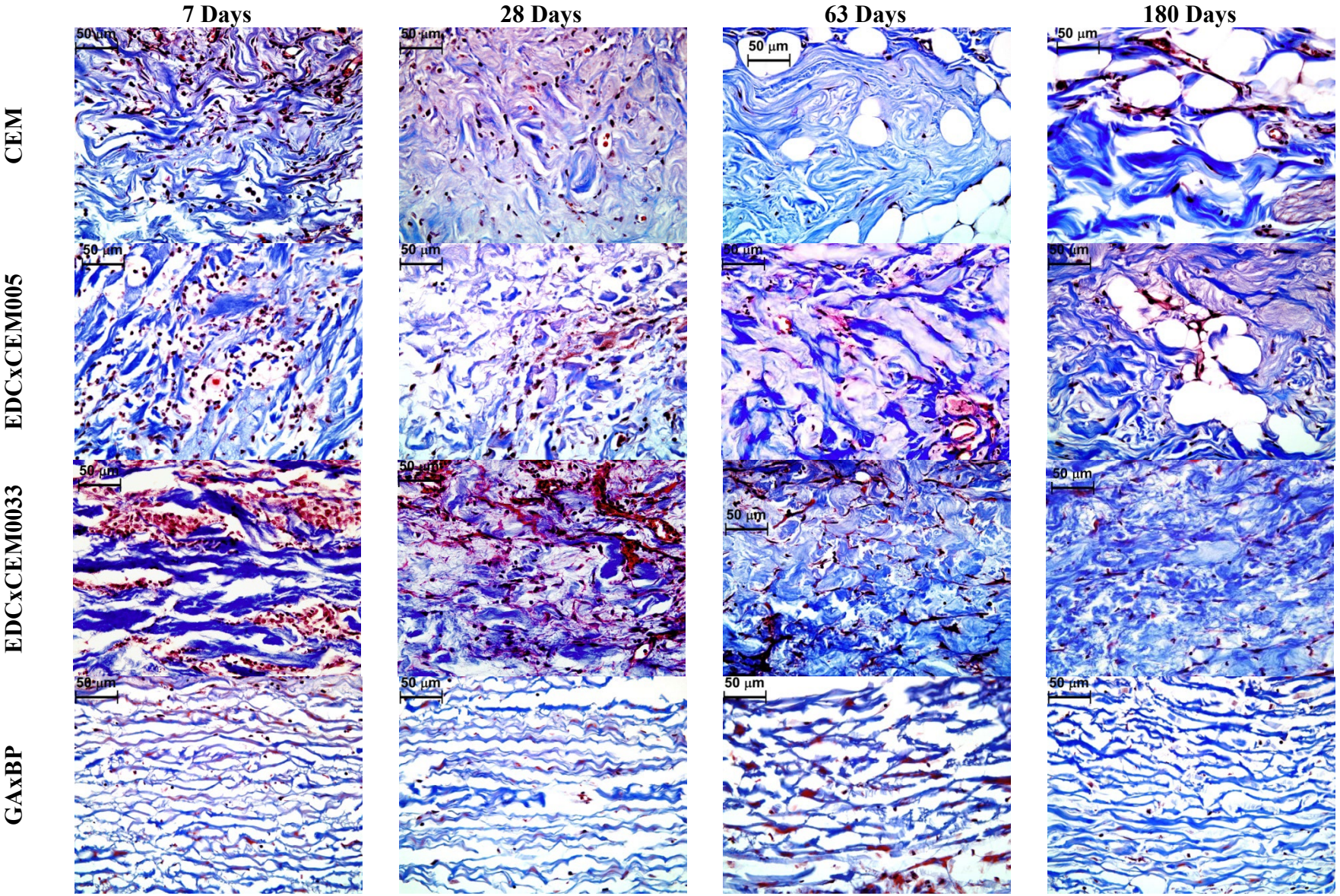

Figure 3: Masson's Trichrome stained histology sections showing the implant area for the different implants as a function of time.

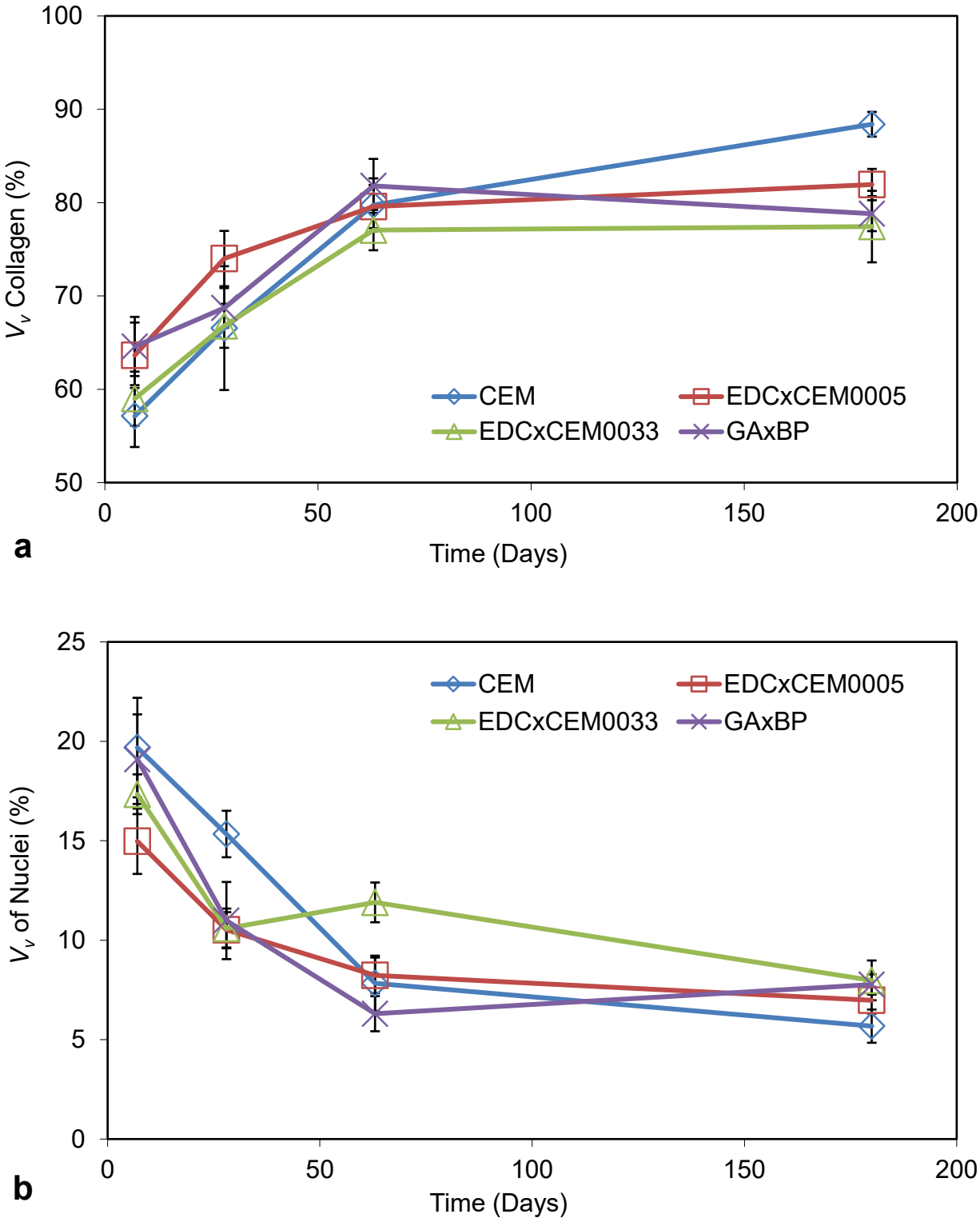

Figure 4: Volume fractions (V_v) of tissue components in the fibrous tissue surrounding the different implants: a) Collagen, b) Nuclei, c) Cytoplasm and d) Blood Vessels, as a function of time.

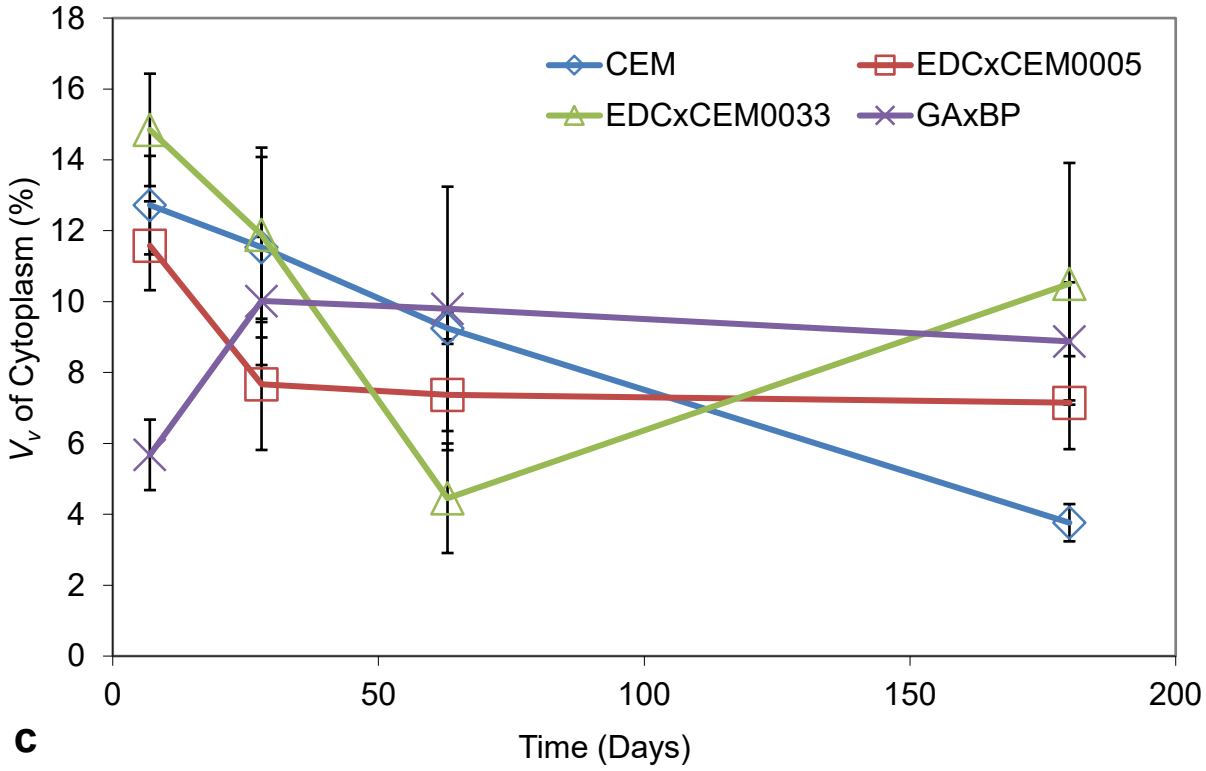

c

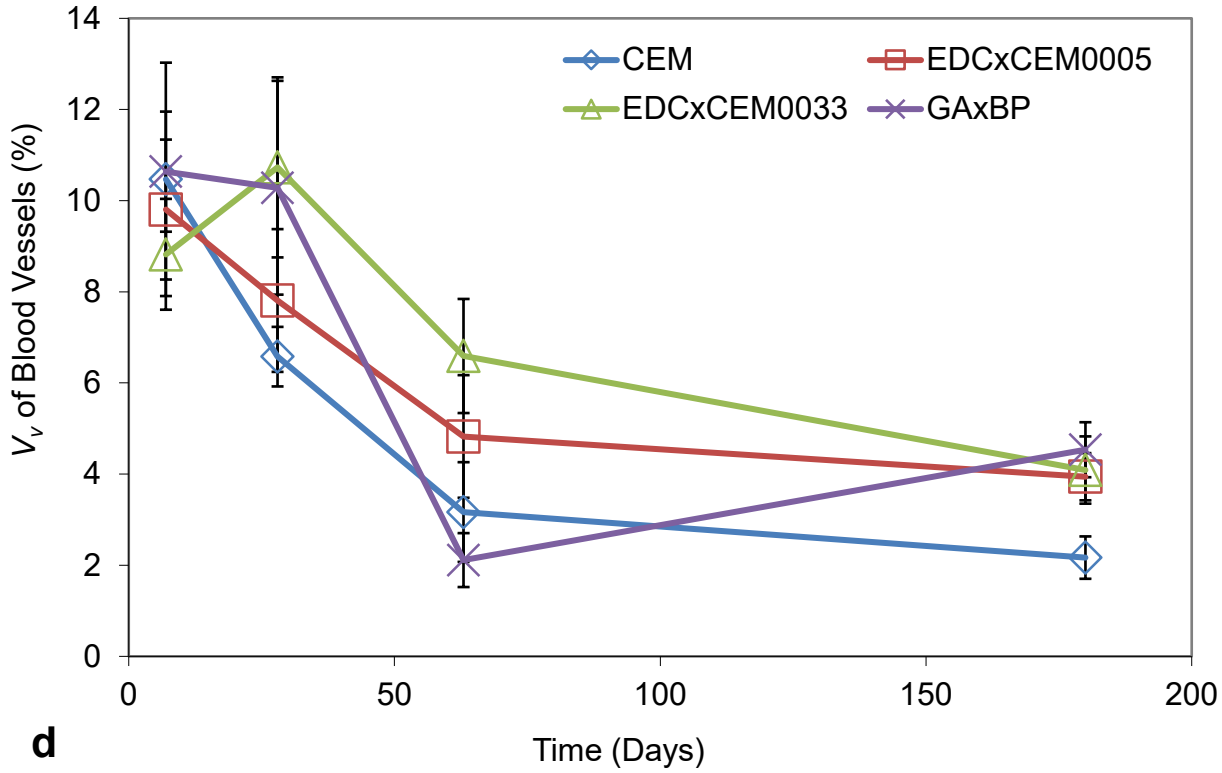

d

Figure 4: (*continued*)

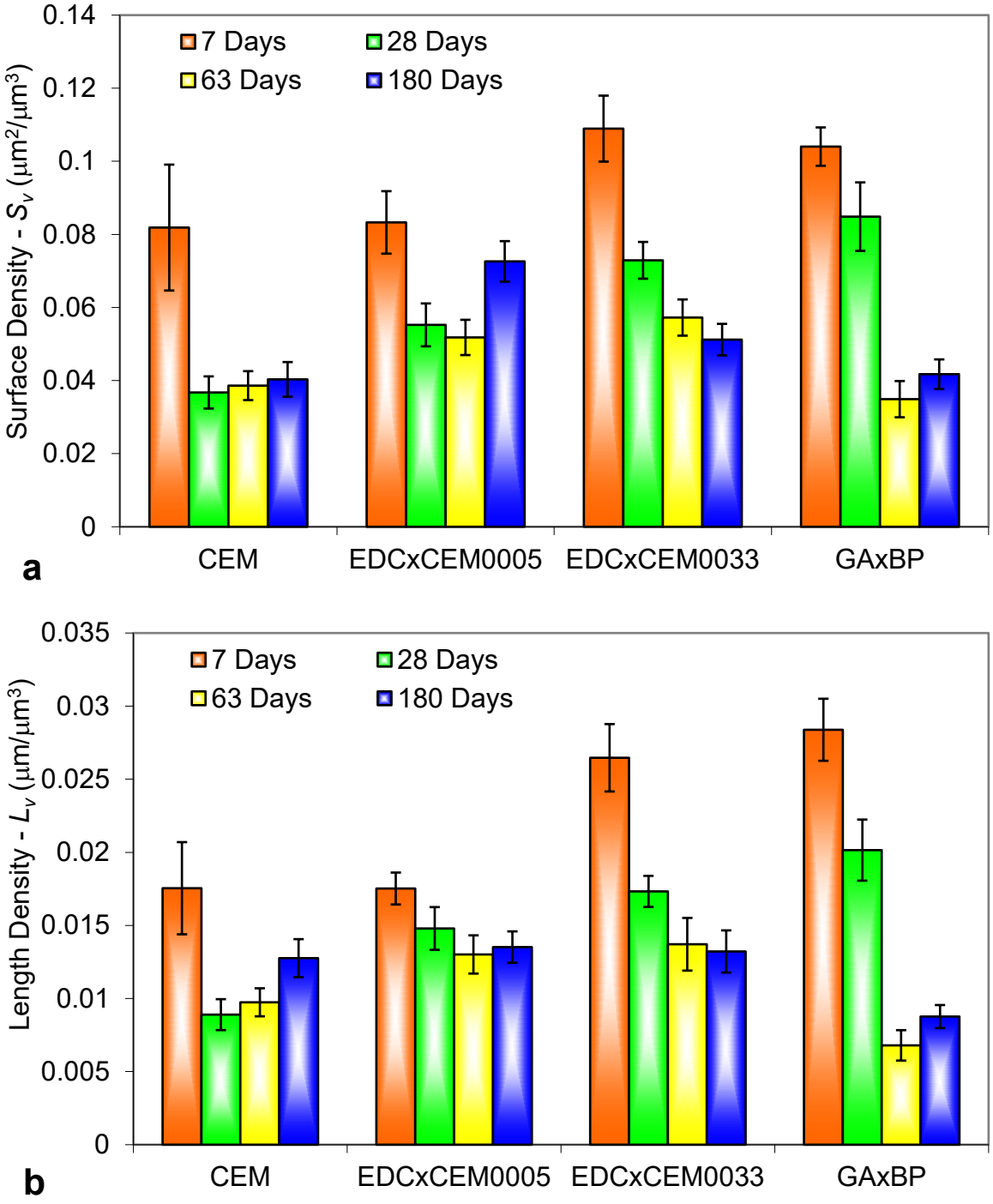

Figure 5: Blood vasculature in fibrous tissue surrounding the implants quantified using stereology on MT stained histology sections: a) surface density (S_v, *surface area of blood vessels per unit volume*) b) length density (L_v, *length of blood vessels per unit volume*) and c) radius of diffusion (R_{diff}, Radial diffusion distance between blood vessels).

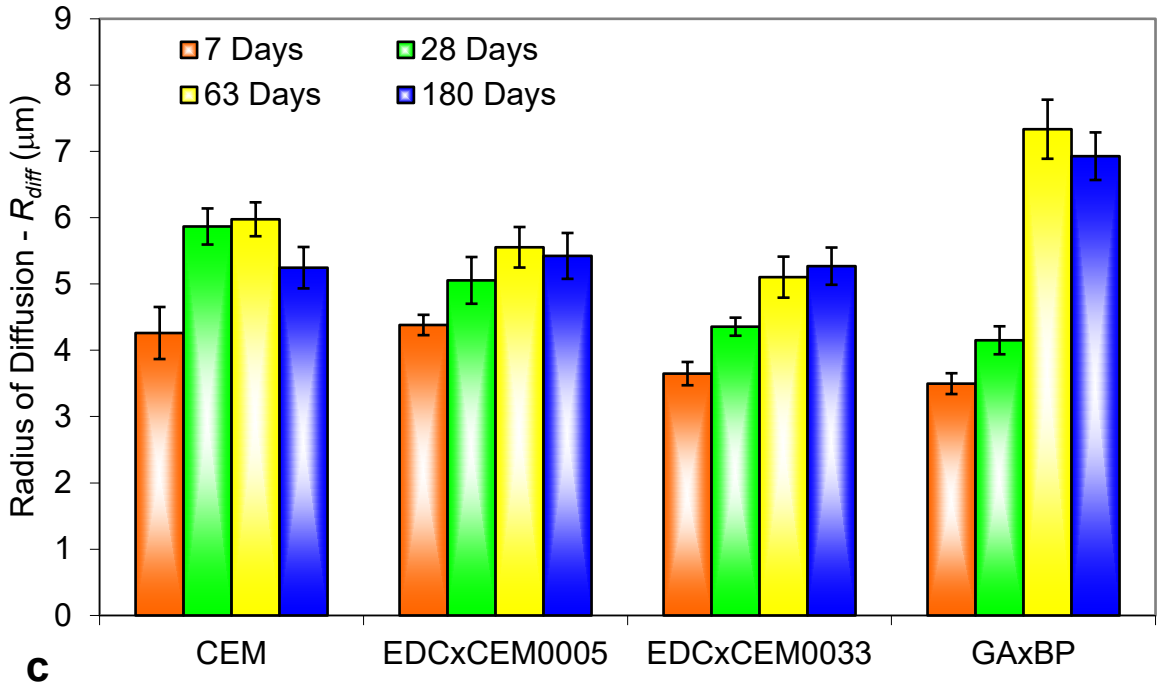

Figure 5: (*continued*)

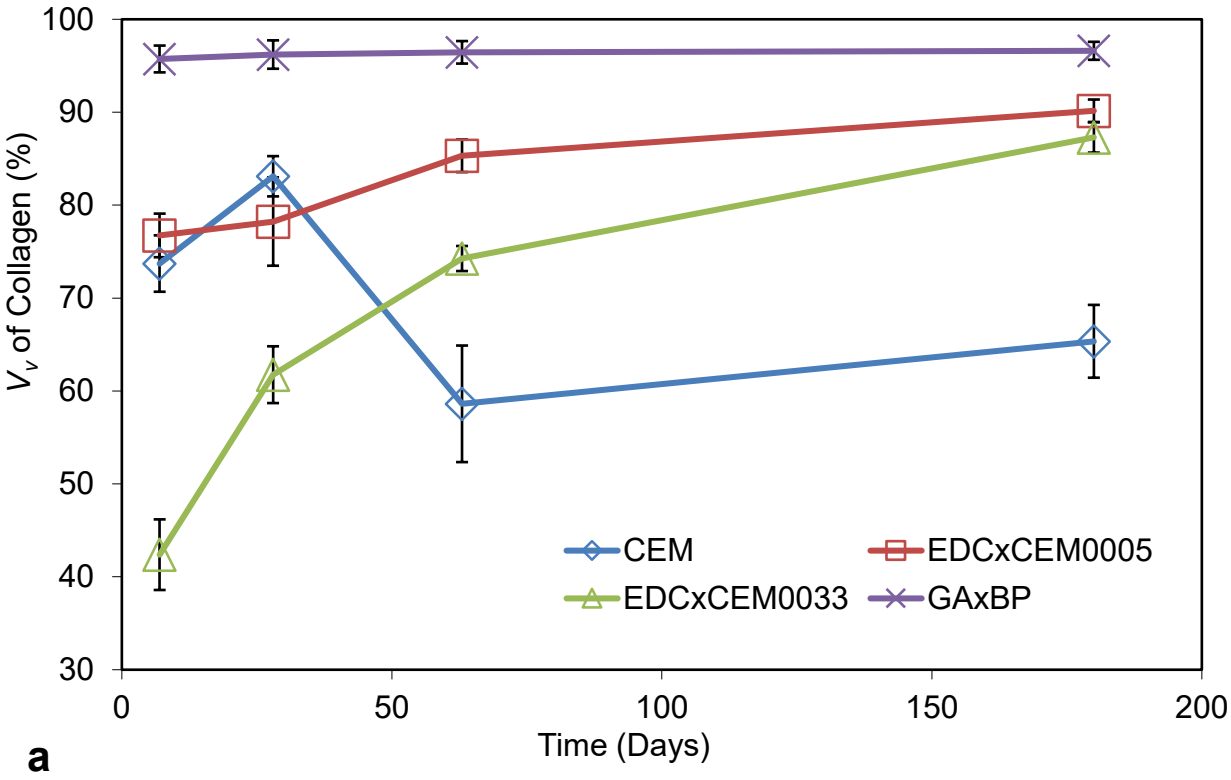

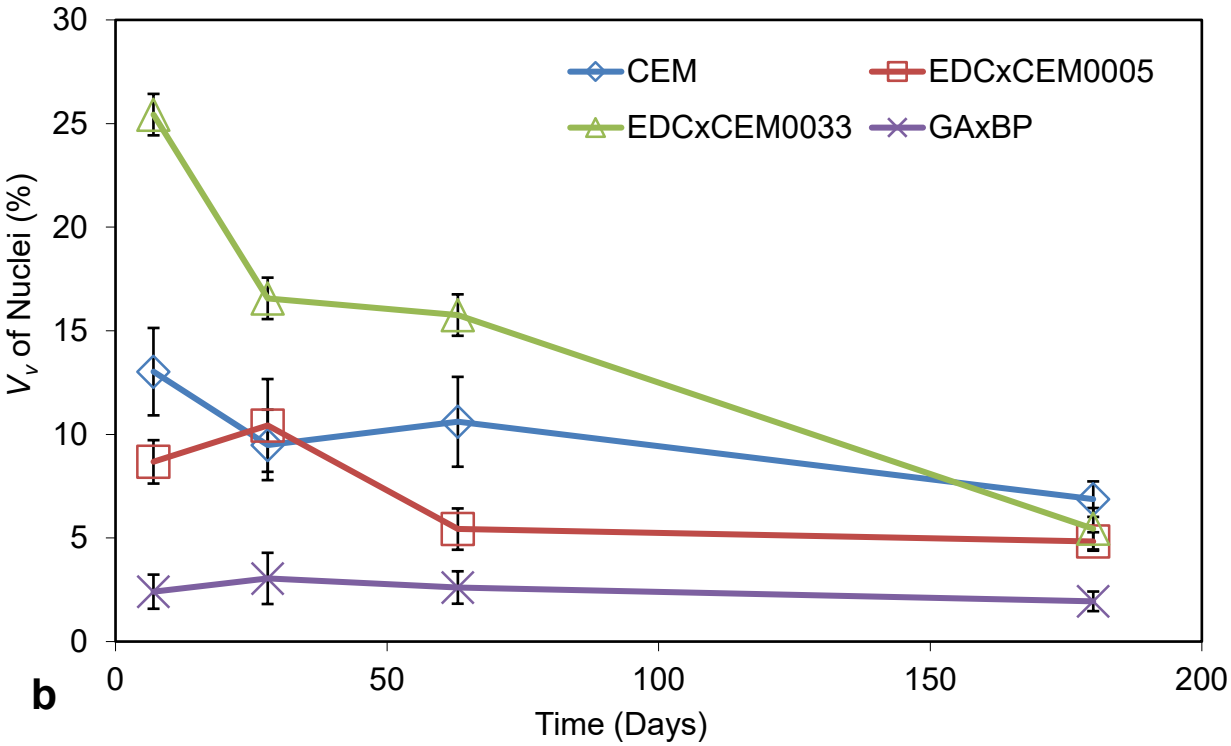

Figure 6: Volume fractions (V_v) of tissue components: a) Collagen, b) Nuclei, c) Cytoplasm and d) Blood Vessels, within the implant area for the different scaffolds, as a function of time.

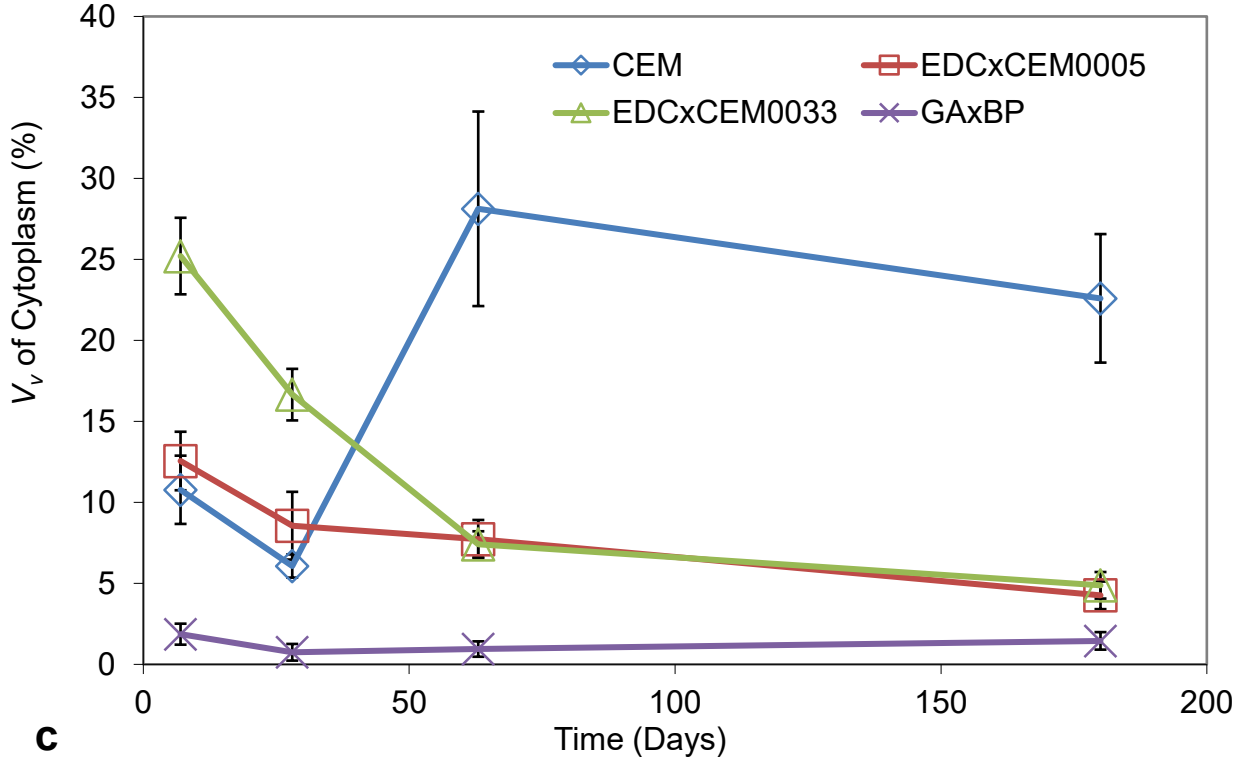

c

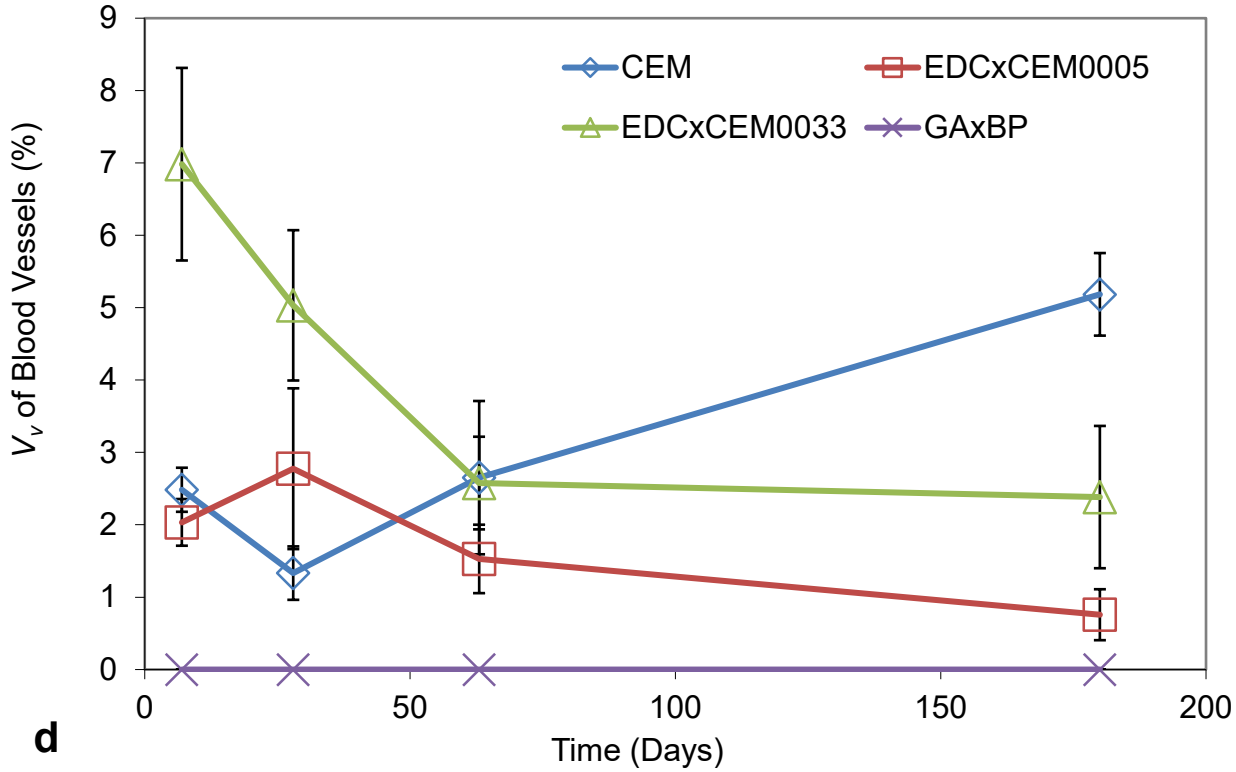

d

Figure 6: (*continued*)

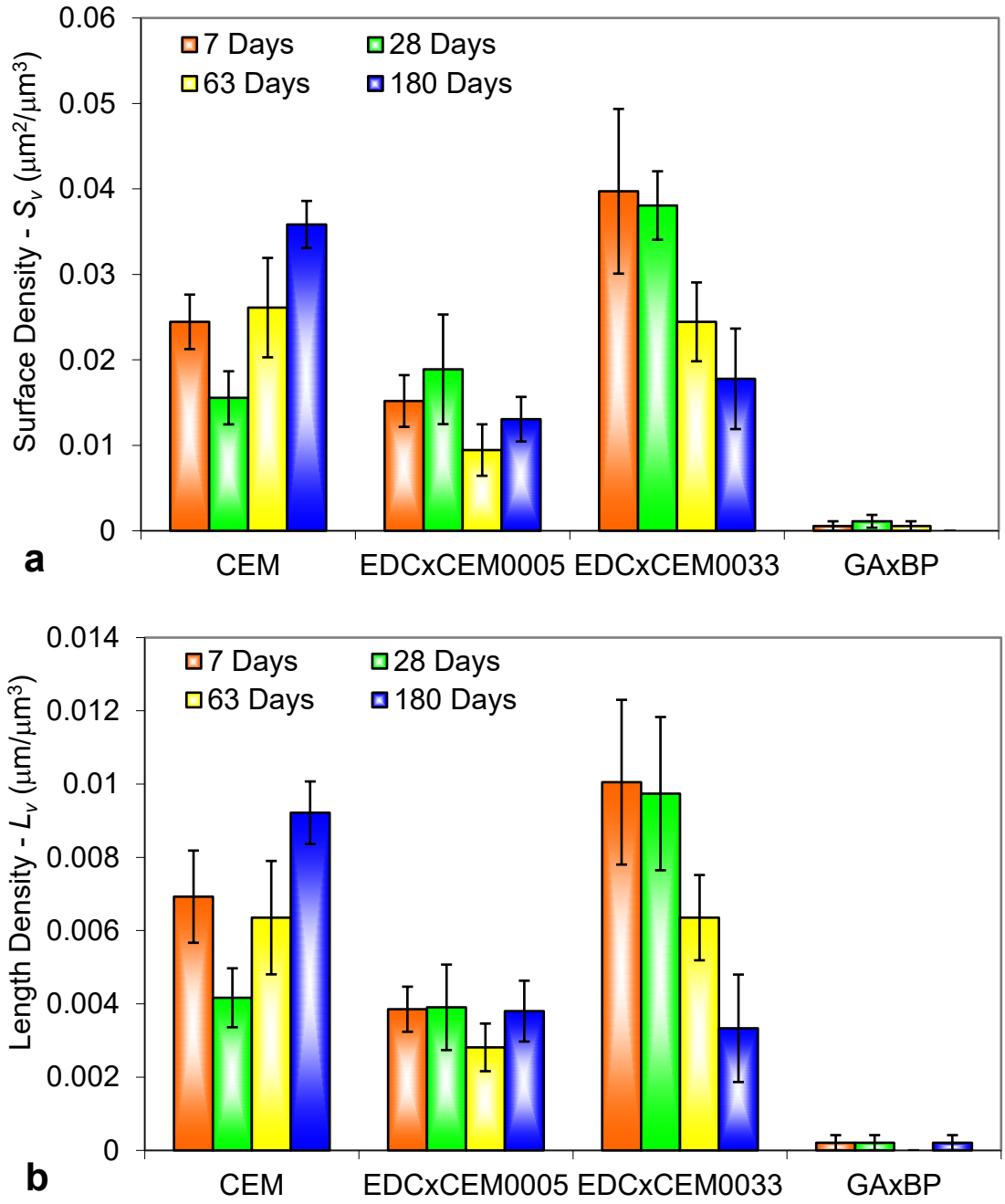

Figure 7: Blood vasculature in the implant area quantified using stereology on MT stained histology sections: a) surface density (S_v, *surface area of blood vessels per unit volume*) b) length density (L_v, *length of blood vessels per unit volume*) and c) radius of diffusion (R_{diff}, Radial diffusion distance between blood vessels).

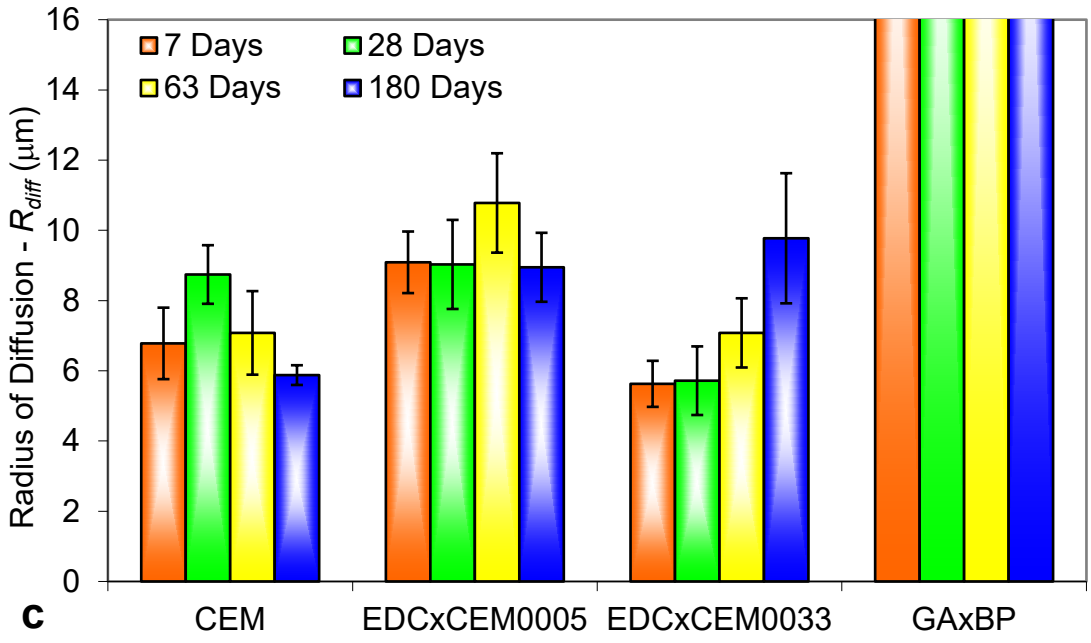

Figure 7: (*continued*)

Table of Content Graphic

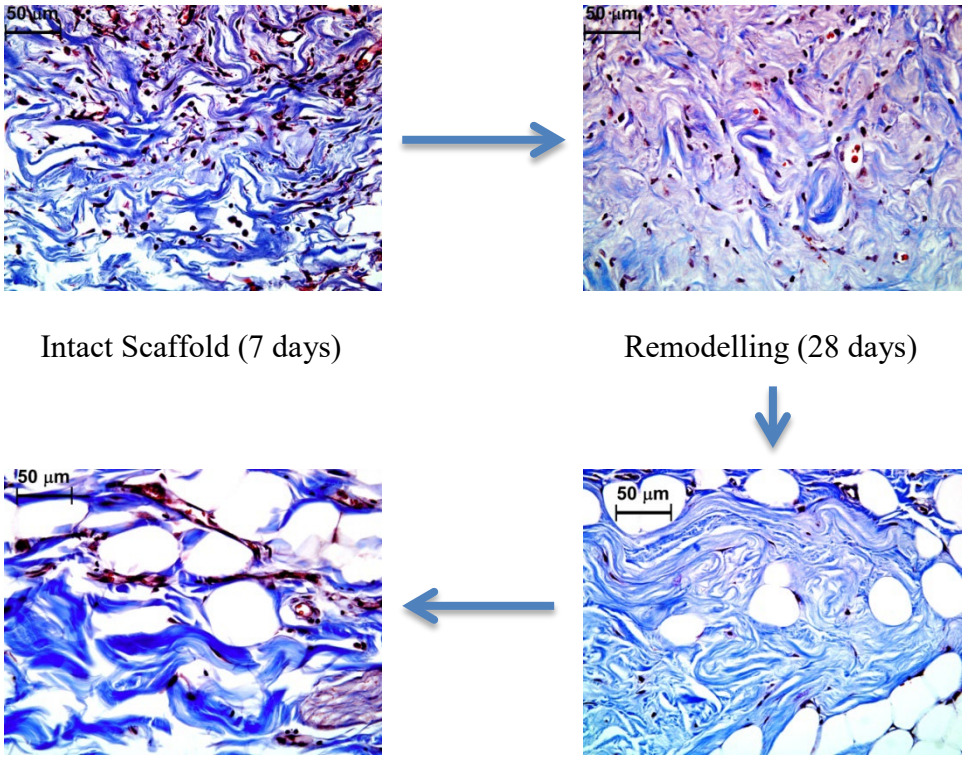

Non-crosslinked CEM showed the phases of 1) granulation tissue deposition within its porous network, 2) resorption of scaffold, 3) concomitant replacement with host tissue (remodelling) and 4) restoration of native adipose tissue composition. The phases were significantly delayed even with minimal crosslinking using EDC.